Hysteretic properties of a two dimensional array of small magnetic particles: a test-bed for the Preisach model

Gábor VÉRTESY

Research Institute for Technical Physics and Materials Sciences
Hungarian Academy of Sciences
H-1525 Budapest, P.O.B. 49, Hungary

Martha PARDAVI-HORVÁTH

Department of Electrical and Computer Engineering
The George Washington University
Washington, DC 20052, USA

Abstract, The magnetization process of a regular two-dimensional array of small, strongly uniaxial single domain magnetic garnet particles, groups of particles, and major loop properties of a "macroscopic" sample, has been investigated experimentally and simulated numerically. These particles correspond to the assumptions of a simple Preisach model. The switching mode is by rotation. Each particle has a square hysteresis loop, with no reversible or apparent reversible component. Requirements of wiping-out and congruency properties are satisfied. From measurements of the up- and down switching fields on individual particles, the major loop can be reconstructed, and it is shown to be in in excellent agreement with the measured one. The transition from individual to collective behavior is smooth and the properties of a system, consisting of 100 particles, correspond to the major loop behavior. The numerically simulated major hysteresis loops agree very well with the measured loops, the switching sequence and the magnetization curve for particle assembly was derived from the calculated interaction fields and found to be in a very good agreement with the measured values, demonstrating the reliability of numerical modeling. A new property, not included into the existing models, is the magnetization dependence of the standard deviation of the interaction field.

Introduction

The predictive power of a theory is especially important for hysteretic phenomena, where the state of the system depends on its history. Among the models, describing hysteretic phenomena, the Preisach model (PM) is one of the earliest and best studied [1]. The original PM assumes the magnetization proceeding by switching of individual two-state particles; and the statistics of this system determines the shape of the macroscopic major and minor loop behavior. It is assumed that each particle switches by coherent rotation, i.e. by the Stoner-Wohlfarth mechanism [2], and there is no

101

reversible or apparent reversible component to the magnetization. The particles might interact magnetostatically, leading to the shift of the individual loops by an "interaction field" H_i. The coercivity of the individual particles, (or critical field) H_c, is determined by physical parameters, as the anisotropy energy, the magnetic moment, and the defect structure. It is assumed that the switching units (particles) are confined to the 4th quadrant, i.e. for the individual rectangular hysteresis loops $H^+ > 0$ and $H^- < 0$, where H^+ and H^- are the up-switching and the down-switching field of a particle. It was shown in [3, 4] that the congruency and the wiping-out properties of minor loops are necessary and sufficient conditions for a hysteretic system to be described by a classical PM. For an assembly of particles both H_c and H_i have a statistical distribution, assumed to be Gaussian, with a mean value $\overline{H}$ and standard deviation σ, leading to the Preisach function in the form of:

$$P(H_i, H_c) = A \exp[-(H_i - \overline{H_i})^2 / 2\sigma_i^2 - (H_c - \overline{H_c})^2 / 2\sigma_c^2]. \qquad (1)$$

The total irreversible magnetization for a system of such particles is given in terms of the experimentally measured parameters H^+ and H^- by

$$M = \int\int D(H^+, H^-) P(H^+, H^-) dH^+ dH^-, \qquad (2)$$

where $D = \pm 1$ gives the direction of magnetization at saturation and the Preisach density function, $P(H^+, H^-)$ corresponds to the number of particles at any given point on the (H^+, H^-) plane. The measured H^+ and H^- are related to H_c and H_i as $H_c = (H^+ + |H^-|)/2$ and $H_i = (H^+ - |H^-|)/2$.

The description and identification of a magnetic material's hysteretic properties in terms of the PM is an ongoing effort. However, most of the important magnetic materials do not conform with the assumptions of the original PM. Therefore significant effort has been devoted to the development of the original model [4,5,6]. At the same time, the experimental study of a hysteretic system, corresponding closely to the assumptions of the classical PM is interesting from the point of view of testing those assumptions and, possibly, describing some properties, not taken into account even in the modified PMs. Magnetic recording is moving toward tremendous recording densities. A possible candidate system for the high density recording media, might be a regular two-dimensional array of very small magnetic particles. The properties of such a system are very close to the original PM, thus giving a direct significance to the investigation of such systems.

The motivation for the present research was to study the properties and the validity of the original PM on a simple model system, corresponding to the assumptions of the simple PM. The hysteretic properties of a simple, two-dimensional system of small single domain,particles are studied and compared to the predictions of the original PM.

1. Experiments

A 3 μm thick single crystalline magnetic garnet film of magnetically diluted $Y_{3-x}Bi_xFe_{5-y}M_yO_{12}$ (YIG), (M=nonmagnetic ion) grown by liquid phase epitaxy on a [111]

oriented non-magnetic garnet substrate, has been etched into a 2D array of 42 μm square pixels, separated by 12 μm wide grooves. Each pixel corresponds to a single particle. The excellent topographical uniformity of the particles, i.e. the perfections of corners and edges is evident from SEM investigations (Fig. 1). Epitaxial garnets are known to have the lowest crystalline defect densities; and optical and scanning electron microscopy observations also revealed the lack of any visible defect in the material.
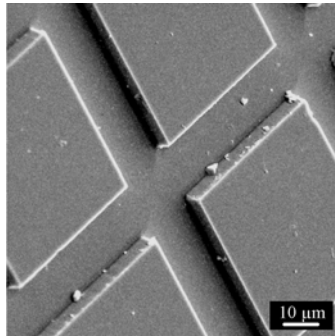

Fig. 1. Detail of the 2D array of garnet particles (SEM)

Experiments were performed on an assembly of up to several thousand garnet "particles". These particles are small *magnetically,* despite of their relative large physical size, because their magnetic properties correspond to the conditions necessary for single domain particles. The magnetooptically active transparent epitaxial garnet film, grown on a transparent substrate, permits direct visual observation via the magnetooptical Faraday effect, with simultaneous electrooptical recording of the state of the pixels (picture elements in optical readout).

The mean values of magnetic parameters of the whole sample were determined in a vibrating sample magnetometer (VSM). The magnetization of the sample, $4\pi M_s = 160$ G, is very low, while the uniaxial anisotropy field $H_u = 2$ kOe. As a result, the particles have high $Q = H_u/4\pi M_s > 10$, ensuring that there are only two stable magnetic states, either "up" or "down" along the easy axis, normal to the film plane (black and white magnetooptic contrast). Each particle has a rectangular hysteresis loop, and the switching of the whole system proceeds by consecutive switching of particles. The squareness of the major hysteresis loop $M_r/M_s = 1$, the average switching field, $H_c = 280$ Oe. Group of pixels and their gradual switching in a magnetic field, applied along the easy axis, i.e. normal to the film, are shown in Fig. 2.

Hysteresis loops of individual pixels and groups of pixels have been measured with an optical magnetometer operating on the principle of Faraday effect. The light from a halogen lamp after a polarizer is focused onto the sample. After passing through the transparent magnetooptic material, the plane of polarization of the light is rotated, depending on the magnitude and the direction of the magnetization. The intensity of the transmitted light after an analyzer is proportional to the magnetization and it is measured by a photomultiplier. The sample is placed in the magnetic field of magnetizing coils, and/or of an electromagnet. The field is oriented along the film normal. Placing a microscope objective after the analyzer, the enlarged picture of the sample is obtained in the image plane of the objective.
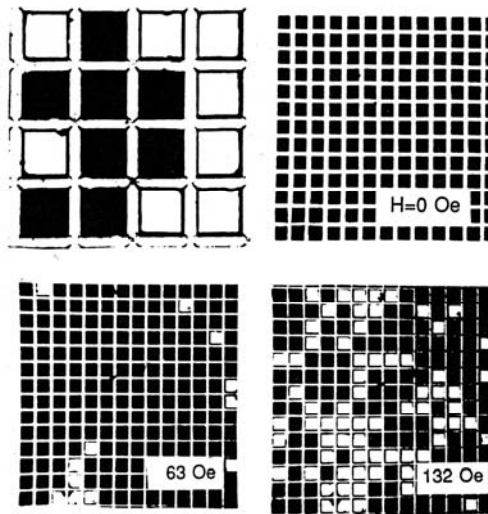
Fig. 2. Microphotographs (Faraday effect, polarized light) of the sample in different states of magnetization. Pixels magnetized "down" are black. Detail of the structured epitaxial garnet film (upper left), and the magnetization process of an assembly of pixels in increasing magnetic field, starting from negative saturation with all pixels dark; in H=0 the remanence is 1; pixels switched to the state of opposite magnetization in the given field have a light contrast
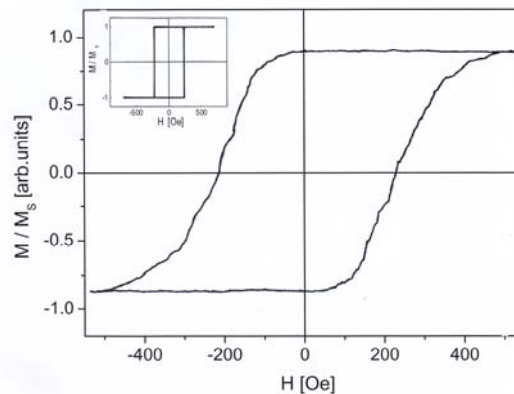

Fig. 3. Major hysteresis loop of several hundred pixels, and the hysteresis loop of a single pixel (insert) of the structured garnet sample

By masking the picture in the image plane, any individual pixel of any group of pixels can be chosen for the measurement of the hysteresis loops. If the sample is projected onto a screen in the image plane, the actual magnetic state of the environment can be monitored simultaneously with the measurement. The light, after passing through the mask is focused onto the photodetector. The hysteresis curve of individual pixels (or groups of pixels) is obtained by measuring the intensity of the light after the analyzer as a function of the external magnetic field.

The major hysteresis loop of several hundred pixels, measured in the optical magnetometer, is shown in Fig. 3. This curve fully corresponds to the major loop, measured in the VSM, however, the large paramagnetic contribution from the substrate is eliminated in this case. The measured hysteresis loop of an individual pixel is also shown in the same figure, as an insert. The loop is square, there is no reversible contribution to the magnetization.

2. Switching properties

Counting the number of black and white pixels switched in a given field H_n is, according to (2), equivalent to determine the actual magnetization state. When the magnetization of individual pixels is measured magnetooptically starting from saturation, it is observed that individual pixels switch abruptly, resulting in perfectly rectangular loops, as seen in Fig. 3 (insert). However, the upper and lower switching fields, H^+ and H^-, might differ from each other due to interaction with surrounding pixels. In the absence of the interaction, there is still a distribution of the switching fields due to defects and irregularities created during processing of the sample. Fig. 4 shows the distribution of the up-and down switching fields on the Preisach plane for 250 pixels, confirming that the system's Preisach function is confined to the 4th quadrant. Here each point on the (H^+,H^-) plane corresponds to one pixel.
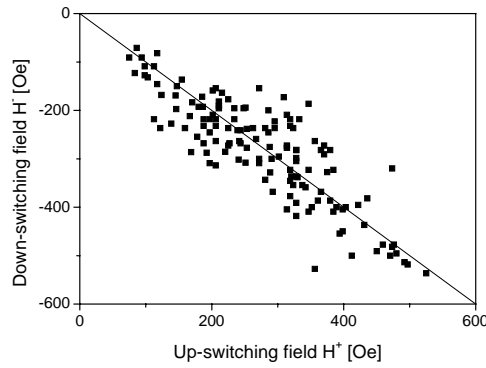
Fig. 4. Distribution of up and down switching fields (H^+ and H^-) on the Preisach plane, as measured from individual hysteresis loops of 250 pixels

Measurement of switching curves on single particles yields H^+ and H^- data for the reconstruction of the major loop from the properties of individual particles. From the statistical analysis of our data, it is concluded that the distribution of the coercivity of individual pixels is Gaussian:

$$P(H_c) = C \exp[-\frac{(H_c - \overline{H_c})^2}{2\sigma_c^2}]$$ (3)

and the mean value corresponds to the major loop coercivity. The mean value of coercivity of the assembly of pixels, $H_c = (H^+ - H^-)/2$ (halfwidth of the individual

105

hysteresis loops) and of the interaction field $H_i = (H^+ + H^-)/2$ (shift of the loops), and the standard deviation of the coercivity and of the interaction field, σ_c and σ_i, have been determined by a numerical fit to a Gaussian distribution in form of (1). The mean value of coercivity $H_c = 258$ Oe and the standard deviation $\sigma_c = 85$ Oe. The value of H_c is in good agreement with the value determined from the major loop measurements.

The average coercive field of an assembly of about 9-16 particles is approaching the major loop coercivity, however, its standard deviation σ_c approaches its limiting value only for a larger number of particles, as shown in Fig. 5. It is seen that σ_c depends strongly on the number of measured particles.
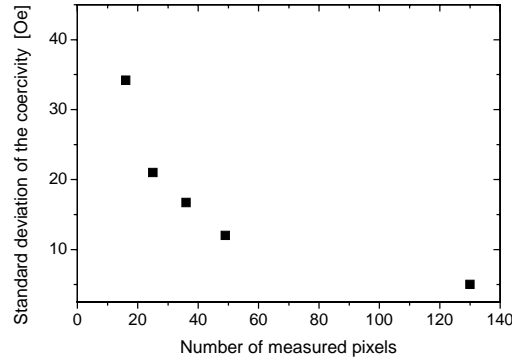

Fig. 5. The standard deviation of the measured coercivity

The particles are physically separated, interacting only magnetostatically. Individual loops are shifted due to this interaction. The measured distribution of interaction fields of individual pixels closely follows a Lorentzian distribution:

$$P(H_i) = \frac{A}{1+[(H_i - \overline{H_i})/\sigma_i]^2}$$ (4)

The mean values of the interaction field is centered around zero, $H_i = 0$ Oe, having a very low standard deviation $\sigma_i = 9$ Oe. It has to be noted that the fit is also good for a Gaussian distribution, the difference being in the slightly wider tails of the Lorentzian, but for more than about 100 particles the Lorentzian is always the best fit.

The measurements of single pixel hysteresis loops always started from saturated state. However, when the measurements started from a state of different magnetization, it was observed that the standard deviation of the interaction field σ_i depends on the actual magnetization:

$$\sigma_i(M) = \sigma_i(0) - \frac{\partial \sigma_i}{\partial M} M.$$ (5)

This property is not included into any of the existing hysteresis models. Eq. (5) is a first-order approximation to this dependence [7], which well describes the measured behavior is shown in Fig. 6. This effect is pronounced in the 2-D case, because the interaction with neighbors in different states can be "magnetizing" or "demagnetizing", depending on the actual magnetization state of the neighbors.. Around negative saturation, any particle switching "upward" has a uniform neighborhood, with all particles being in the "down" state and acting on the "test" particle with an effective positive interaction field, thus assisting the change of the magnetization state of the test particle. In this case σ_i has the smallest value. In contrast, around the demagnetized state, the variety of all possible combinations of "up" and "down" neighbors is the largest (5625 possible states for 25 neighbors) and σ_i reaches its maximum value. The actual magnitude of σ_i was calculated statistically in [8]. The interaction fields, calculated from exact surface integrals for the magnetostatic interaction of individual square pixels are in excellent agreement with measured values (details are given in Section 5.).
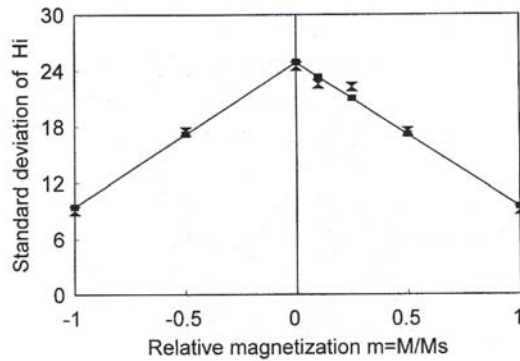

Fig. 6. Magnetization dependence of the standard deviation of the interaction field

The problem with the hysteresis modeling is related to the facts that the magnetization is not only non-linear, but it is a multivalued function of the magnetic field. Its value depends on the prehistory of the material. For the case of the array of pixels, it is easy to understand and measure this dependence based on the state of magnetization of the pixels, surrounding a selected "test" pixel. Starting from negative saturation and observing the switching of any given pixel, the switching fields differ depending on the state of it neighbors. The interaction field originates from the demagnetizing field of neighbors acting on the test (central) pixel. The effect of the state of the magnetization of the surrounding pixels on a given test pixel gives a linear dependence, which is characterized by $dH_i/dn = 26$ Oe/pixel slope, where n is the number of first neighbors being already switched [9]. This value can be compared with $H_D = 32$ Oe, the demagnetizing field estimated for an ablate ellipsoid of rotation [2]. The effective field acting on the central pixel is the externally applied field reduced by this amount for each neighbor in the oppositely magnetized state (OMS). The switching field of the observed (central) pixel depends not only on the number of the neighbors with opposite magnetization, but it depends on their position, too. There are two kinds of first neighbors: four of them are located side-by-side at a distance of $d = 54$ μm, four are in

107

corner positions, their centers at $\sqrt{2}d$. The difference between the value of the switching fields has been found experimentally, depending on the configuration of the first neighbors in OMS. For $n = 1$, i.e. there is one neighbor in OMS, when it is side-by-side $H^+ = 262$ Oe is the applied field needed to switch the central pixel. When the neighbor in OMS is in a corner position $H^+ = 220$ Oe is sufficient to switch the central pixel. The down-switching field values, H^- depend also on this geometry. The resulting interaction fields (shift of the hysteresis loops) are 81 Oe and 48 Oe for the two cases.

These observations clearly show that the properties of this simple system, consisting of single domain particles, having individual rectangular hysteresis loops and a fully reversible major loop, closely correspond to the assumptions of the classical PM. Due to the regularity of the system, numerical calculation of the interaction field is straightforward [10]. The Preisach function and its integral (the total magnetization) can be obtained directly by counting the number of particles in up and down magnetized states. The system is completely restrained to the 4th quadrant of the Preisach plane. A new property, not included into the existing models, is the magnetization dependence of the standard deviation of the interaction field. Further aspects of the behavior of this system are discussed in the next paragraphs.

3. Behavior of minor loops

The properties of minor loops of the above described model system were experimentally studied in [11]. Fig. 7 shows the major loops for about 120 pixels, what coincides with the major dc remanence loop, because there is no reversible contribution to the magnetization. The initial magnetization curve, starting from ac demagnetized state (a), and several minor loops (b), illustrating the development of the major dc remanence loop, are also shown. The remanence is equal to the magnetization value, $M(H) = M_r$, and the remanence coercivity is equal to the major loop coercivity, $H_c = H_r$.
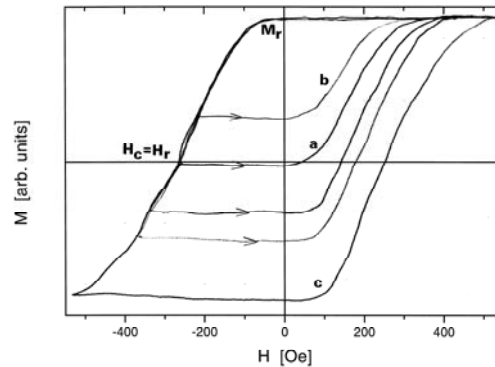

Fig. 7. Magnetization curves for a group of pixels. a) remanence curve; b) minor loop for dc remanence measurements; c) major loop

Fig. 8 illustrates the wiping-out property, i.e. the return of the magnetization after traversing a minor loop to the same major loop value (loss of memory prehistory) for 81 pixels of the same 2D patterned film. The individual Barkhausen jumps are clearly visible on the original records. The minor loops are straight lines. The cycling of the
108

field between the major loop and $H \cong 0$ does not lead to switching of any particles, as the magnetization is not changing because $H_{max}^{-} < 0$. However, upon decreasing the field further, irreversible switching of pixels begins, and depending on the number of pixels switched, the minor loops get wider.
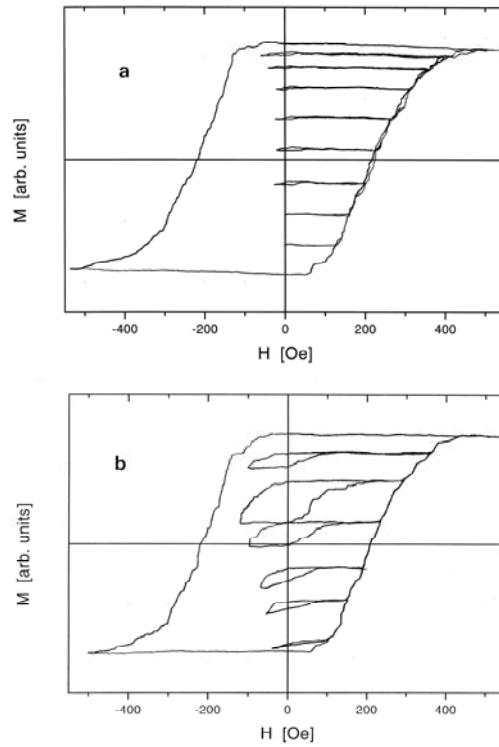
Fig. 8. Wiping-out property for 81 pixels of the 2D array of garnet particles, switching by rotation of the magnetization. a) the field is reversed before switching starts; b) the number of pixels switched depends on the reverse field

Starting from the same point on the major loop, and controlling the end-field of minor loops, minor loops of peculiar shapes can be prepared. The area of the loops is equal to the number of the pixels switched "back and forth" during the cycle of the minor loop. This number is different for loops with different "average" magnetization at their center. This has a direct consequence as the non-congruency of the minor loops. The distribution of the up- and down switching fields of the pixels is directly responsible for this behavior [9,12].

Fig. 9 shows the congruency of minor loops for the structured sample, when the field is cycled around $H = 0$. However, congruency is not observed when minor loops are centered at H ≠ 0. In this case the minor loops are narrower on moving away from the $M = 0$ axis. The measurements show as well that there is no accommodation of minor loops takes place (shift of loops upon repeating).
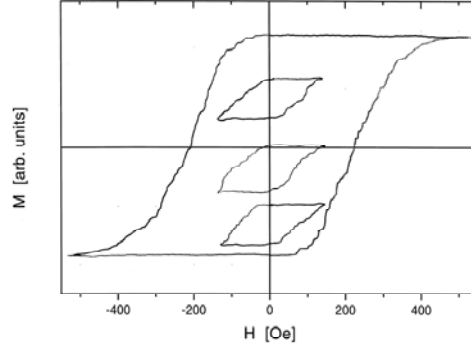
Fig. 9. Congruency property for the same 81 pixels, upon cycling the field around H=0

4. Major loop reconstruction from switching of individual particles

A numerical model has been built to reconstruct the major loop for these assemblies [13]. Measurements and simulations are based on three different size pixel groups, containing 5x5, 7x7, and 9x9 pixels. The external field H_{app} is applied normal to the sample plane (z easy axis). The magnetization is along the film normal. The pixels interact magnetostatically. The effective field acting upon a pixel depends on the state of the neighbors. Assuming the external magnetic field is in the $+z$ direction, each neighbor with a magnetization along $+z$ will have an effective demagnetizing effect on the neighbors having $+M$, i.e., reducing the internal field H_{in}, and a magnetizing effect on neighbors with $-M$.

Due to the nonelliptsoidal shape, the internal field is not uniform, even when $H_{app} \geq 4pM_s$. The reason is that the demagnetizing field, acting on each pixel from all other pixels, is not uniform [14]. The interaction tensor elements' $D(|i-i_0|,|j-j_0|)$ at each pixel (i_0, j_0) from any other pixel (i, j) were calculated using the finite difference method (FDM), either by calculating the surface integrals or by the dipole approximation [8], then the effective interaction field at any pixel, located at (i_0, j_0), from all other pixels can be obtained

$$H_i(i_0,j_0)=4\pi M_S\sum_{i,j}\Lambda\ D(|i-i_0|,|j-j_0|) \tag{6}$$

where $\Lambda=\pm1$, depending on the orientation of M_s [15]. The internal field acting on each individual pixel can be calculated by

$$H_{in}(i_0,j_0)=H_{app}-H_i(i_0,j_0)=H_{app}-4\pi M_S\sum_{i,j}\Lambda\ D(|i-i_0|,|j-j_0|) \tag{7}$$

Once there is a pixel whose state has been changed, the magnetization and the distribution of the interaction field changes. From Eq. (7) it follows that the distribution of the internal field also changes, and the new internal field $H'_{in}(i_0,j_0)$, acting on each individual pixel, can be calculated by

110

$$H'_{in}(i_0, j_0) = H_{in}(i_0, j_0) + 8\pi M_S \, D(|i_0 - i_s + 1|, |j_0 - j_s + 1_s|) \tag{8}$$

where (i_s, j_s) is the location of the pixel which just switched its state. Using the formula, the simulation time can be drastically reduced, especially for the three-dimensional (3-D) case.

There are two ways to obtain the coercivity distribution $H_c(i_0, j_0)$. Based on the measurement of switching fields of individual pixels, it is known that the coercivity of this system has a Gaussian distribution (see above), with known mean value and standard deviation. The coercivities can be generated based on these two values and these values are assigned to each individual pixel randomly. Another way is to use the measured coercivity of each pixel.
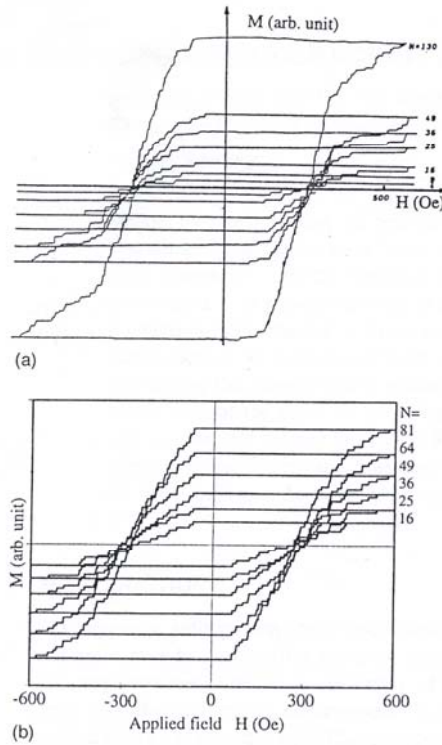

Fig. 10. Major hysteresis loops for different groups of pixels: (a) measured, (b) simulated

Changing H_{app} between negative and positive saturation numerically, the magnetization curve, i.e. the major loop M vs H_{app} is reconstructed from the sequence of the individual switching events. The measured major hysteresis loops for different groups of pixels are shown in Fig. 10(a). The results of simulation, corresponding to these measurements, are shown in Fig. 10(b). The correspondence between the two sets of data is very good. The simulation is based on measured pixel coercivities. Each pixel was assigned its measured H_c. If the coercivities are assigned randomly, the loops do not change much,

111

but the sequence of switching is different for a pixel group. Figure 10(b) shows the switching sequence for a 9x9 pixel group using the measured H_c.

These 9x9 pixels are part of thousands of pixels in the film. So, they are not isolated. Their switching is affected by the pixels beyond the measured 9x9 pixels. In order to examine the difference between the embedded case, where the interaction and the state of the neighbors are taken into account, and the isolated case when the effect from any outside pixels is ignored, an assembly of 5x5 pixels, either isolated, or embedded into a 9x9 group, was measured and modeled. The interaction with all pixels in the 9x9 group are taken into account when calculating the switching of 5x5 pixels. The isolated loop is somewhat more steep than the embedded, showing the effect of the boundary conditions. However, according to Ref. [14], the interaction fields from outside the 9x9 pixels contribute only 3% to the fields from the pixels inside of the 9x9 group.

The model and the simulation are very reliable and efficient to reconstruct the major hysteresis loop based on the calculated interaction fields and measured major loop coercivity and its standard deviation. More strong evidence verifies our model and simulation when comparing the average measured value of the coercivity for the 5x5 pixels: H_{avg}=234 Oe, which agrees well with the simulation for the isolated 5x5 group, H_{isol}=233 Oe. As it is expected, the embedded loop simulation gives a result H_{emb}=217 Oe, very close to the measured major loop H_c=213 Oe.

The very high Q value, i.e. the measure of strong uniaxiality, makes this system against thermal fluctuations extremely stable. Therefore, thermal fluctuations, leading to fluctuating values of individual switching fields, are not included in the present analysis. This is the reason that the calculated switching sequence is always the same for the same group of pixels. However, repeated measurements of major loops consistently show the same switching sequence, indicating that for the given system the dominant factor, governing the shape of the major loop, is the distribution of the coercivities of the individual particles. This coercivity, in turn, is determined by the microstructure and the defects of the particles.

5. Interaction effects

The magnetostatic interaction between the elements of the two-dimensional array can be investigated by taking similar assumptions as described in the previous section. The effect of the magnetic state of the first 5 coordination shells (24 pixels) was investigated experimentally and numerically [8]. The demagnetization tensor for an individual pixel was computed, followed by calculation of the interaction field acting on the center pixel from its neighbors. The relationship between the magnetization state of the neighbors and the interaction field on the central pixel was also calculated using a statistical model.

The model is illustrated in Fig. 11, where r is the distance of the "test" pixel (field point) from the nth neighbor (source point). In the model, five neighbors are considered, at distances from the center pixel of d, $\sqrt{2}d$, $2d$, $\sqrt{5}d$, $2\sqrt{2}d$. The external field is applied normal to the sample plane. The test pixel is at the center of the sample. The total magnetization is given by the difference of the number of "up" and "down" magnetized pixels. The effective field acting on given pixels is the sum of the external field plus the vector sum of the interaction fields from the surrounding pixels.
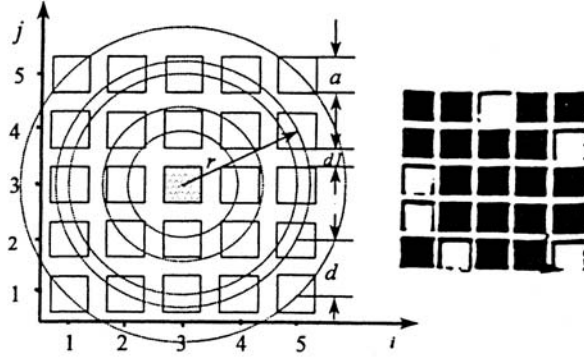
112

Fig. 11. The 2-D array of 25 pixels, corresponding to 5 coordination shells

The demagnetizing tensor D describes the interaction between any two pixels. It can be calculated by a surface integral or using the dipole approximation [10,14,15]. The field at pixel i due to pixel j, H_{ij}, is expressed as:

$$H_{ij} = D(r_{ij}) \bullet M_j \tag{9}$$

where $r_{ij} = r_i - r_j$ is the relative distance between pixels, and M_j is the magnetization of pixel j. In the two dimensional case, the only relevant term is $D_{zz}(i,j)$. That means that the direction of magnetization of pixels and the applied field are normal to the sample plane. The demagnetization tensor element is defined by the surface integral. Expanding the integral into a Taylor series of $1/r_{ij}$ for large r_{ij} the first term gives the dipole approximation:

$$D_{zz}(i,j) = -d^3 / 4\pi r_{ij}^3 \tag{10}$$

where d is the size of the rectangular pixels. Table I shows the values of D_{zz} calculated by these methods. The dipole approximation overestimates the exact surface integral calculation D_{zz} by 17.4% for the first neighbor, and by 1.4% for the second neighbor; the deviation being negligible at larger distances.

Table I: Comparison between the dipole approximation and surface integral for demagnetizing tensor element $D_{zz}(x,y,z)$

Shell	1 st	2 nd	3 rd	4 th	5 th
Distance	d	$\sqrt{2}d$	$2d$	$\sqrt{5}d$	$2\sqrt{2}d$
Dipole	-79.58	-28.13	-9.947	-7.118	-3.517
Surf. Int.	-67.79	-27.73	-9.848	-7.103	-3.513
Error, %	17.4	1.4	1.0	0.21	0.11

The interaction field at the center pixel is equal to the sum of demagnetizing fields from all neighbors. The demagnetizing field from pixel j at pixel i depends on the magnetization:

$$H_D(i,j) = D_{zz}(i,j)\, 4\pi M_j \qquad (11)$$

The magnetization of the garnet sample is $4\pi M_j = 160$ G. The field, acting on the pixel, vs. distance of the neighbors is shown in Fig. 12.
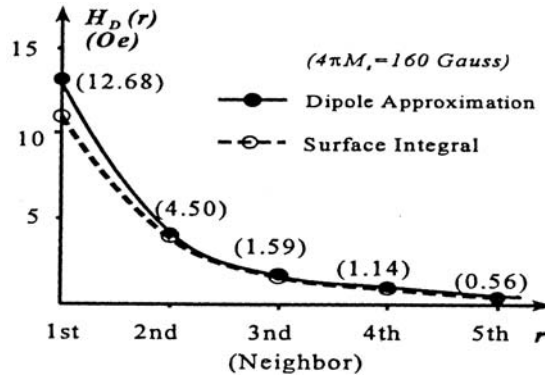

Fig. 12. The distance dependence of the demagnetizing fields at the central pixel, calculated by the surface integral and dipole approximation (The numbers on the curve are the dipole approximation)

The interaction field at a given pixel, originating from all the other pixels is given by

$$H_I = 4\pi M_s\, N_{zz} \qquad (12)$$

where $N_{zz} = \sum\sum D_{zz}(i,j)$, and the sign of $D_{zz}(i,j)$ is determined by the state of pixel j. In fact, N_{zz} is (de)magnetizing factor. The measured up-switching field of the pixel is equal to:

$$H^+ = H_{c0} - H_t \qquad (13)$$

where H_{c0} is the coercivity of central pixel. H_{c0} could only be measured on an isolated pixel, however, it can be determined from the measured H^+ and calculated H_i. For all the 24 neighbors switched "up", in other words, no neighbors in the "down" state, $H_i = -86$ Oe, and $H^+ = 398$ Oe, resulting in $H_{c0} = 312$ Oe for that pixel.

Comparing and subtracting H^+ for different configurations, one can determine the contribution of each neighbor surrounding the central pixel. The slopes of the experimental curves are in good agreement with the numerical model, proving that the contribution from the 4th, 5th and further coordination shells is negligible.

114

It can be assumed that the distribution of the "up" and "down" pixels around the central pixel is random. For the system of 5x5 pixels of Fig. 11, there are 24 neighbors in five shells. Each pixel might be in 2 states. The first shell has 4 pixels; their states may be 0, 1, 2, 3, 4 "up", i.e. five cases. For whole system, there are 5625 possible states of the 24 pixels. The probability of each individual state can be calculated, and the value of the interaction field can be determined. It is trivial, that there is only one state when all 24 pixels are "up", their demagnetizing effect is maximal and equal to the sum from all pixels $H_i = -86$ Oe. In a similar way, when all the 24 pixels are "down", they have a magnetizing effect with , $H_i = +86$ Oe, added to the applied field. The number of cases is the maximum in the demagnetized state, when 12 pixels are "up", and the average interaction field is zero, although the standard deviation of H_t is the maximum, $\sigma_i = 38.81$ Oe. Fig. 13 shows , H_i and σ_i and the calculated probabilities of the statistical distribution.
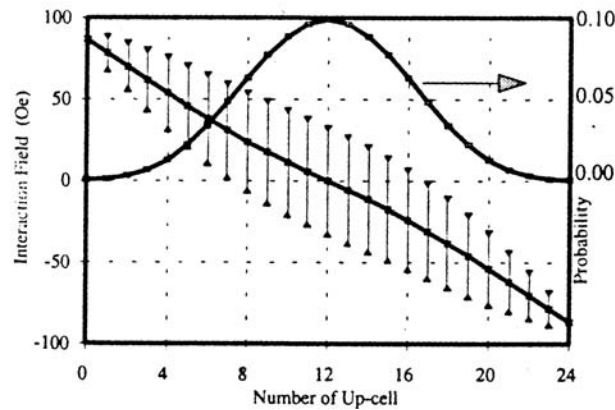

Fig. 13. The mean value and standard deviation of the interaction field at the center pixel vs the number of "up" neighbors, and the probability of having N neighbors magnetized "up"

Conclusion

The magnetization process of a two dimensional regular array of small, single domain, uniaxial magnetic garnet particles, groups of particles, and minor and major loop properties of a "macroscopic" sample have been investigated experimentally in an optical magnetometer. This assembly of particles, interacting magnetostatically, corresponds to the assumptions of a classical PM: the switching mode is by rotation; each particle has a square hysteresis loop; there is no reversible or apparent reversible magnetization. The system possesses the wiping-out and congruency properties, and the Preisach function is confined to the 4th quadrant of the Preisach plane.

The macroscopic major hysteresis loop develops for an assembly of approximately 100 particles, although the major loop coercivity develops much earlier. The distribution of the critical field for switching of the individual particles follows a Gaussian, with a mean value equal to the coercivity of the major loop. The interaction fields are distributed according to a Lorentzian function, with standard deviation strongly depending on the magnetization.

115

A numerical model has been built to reconstruct the major loop for these assemblies. The simulation results agree very well with the measurements. This demonstrates the efficiency and reliability of numerical modeling. Thermal fluctuations, leading to fluctuating values of individual switching fields, are very unlikely for this strongly uniaxial system. This is the reason that the calculated switching sequence is always the same for the same group of pixels. Repeated measurements of major loops consistently show the same switching sequence, indicating that for the given system the dominant factor, governing the shape of the major loop, is the distribution of the coercivities of the individual particles. This coercivity, in turn, is determined by the microstructure and the defects of the particles.

The interaction effects in this 2-D array between a central pixel and the surrounding coordination shells have also been measured. The interaction field and it standard deviation was calculated for all possible random distribution of 24 pixels around the test pixel. The measured and calculated interaction fields for different configurations are in excellent agreement.

Besides the fact that the described system serves as a fine model material for the experimental verification of the validity of the PM, the results are also applicable to very high density magnetic recording, because a promising medium for future extreme high density magnetic storage consists of regular two-dimensional arrays of single domain particle bits in the shape of rectangular platelets or cylinders. Similar treatment can be applied to describe other magnetic devices, such as magnetic random access memories (MRAM) and sensor arrays, are also based on small magnetic particles.

References

[1] F. Preisach, Z. Phys. 94 (1935) 277.
[2] E.C. Stoner, E.P. Wohlfarth, Phil. Trans. Roy. Soc. London A 420 (1948) 599.
[3] I.D. Mayergoyz, Phys. Rev. Len. 56 (1986) 1518.
[4] I.D. Mayergoyz, Mathematical Models of Hysteresis, Springer Verlag, 1991.
[5] G. Bertotti, Hysteresis in Magnetism, Academic Press, 1998
[6] E. Della Torre, IEEE Trans. Audio Electroacoust., 14 (1966) 86.
[7] M. Pardavi-Horvath, E. Della Torre, F. Vajda and G. Vértesy, IEEE Trans. Magn. 29 (1993) 3793.
[8] M. Pardavi-Horvath, G. Zheng, G. Vértesy and A. Magni, IEEE Trans. Magn. 32 (1996) 4469.
[9] M. Pardavi-Horvath and G. Vértesy, IEEE Trans. Magn. 30 (1994) 124.
[10] M. van Kooten, S. de Haan, J.C. Lodder, A. Lyberatos, R.W Chantrell and J.J. Miles, J. Magn. Magn. Mater. 120 (1993) 145.
[11] M. Pardavi-Horvath and G. Vértesy, IEEE Trans. Magn. 33 (1997) 3975.
[12] M. Pardavi-Horvath, IEEE Trans. Magn. 32 (1996) 4458.
[13] G. Zheng, M. Pardavi-Horvath and G. Vértesy, J. Appl. Phys. 81 (1997) 5791.
[14] Y.D. Yan and J. Della Torre, J. Appl. Phys. 67 (1990) 5370.
[15] G. Zheng, M. Pardavi-Horvath and X. Huang, J. Appl. Phys. 79 (1996) 5742.